Research Article

Axolotls' and Mice's Oral-Maxillofacial Trephining Wounds Heal Differently.

Andre Marc Charbonneau[a,b,c], Pirjo Åström [b], Tuula Salo [b,c], Stéphane Roy [d*], Simon D Tran [a*]

[a] Craniofacial Tissue Engineering and Stem Cells Laboratory, Faculty of Dentistry, McGill University, Montreal, Canada, H3A 0C7.

[b] Cancer and Translational Medicine Research Unit, University of Oulu, Medical Research Center Oulu, University of Oulu and Oulu University Hospital, Oulu, Finland

[c] Department of Oral and Maxillofacial Diseases, University of Helsinki, Helsinki, Finland and HUSLAB, Helsinki University Hospital, Helsinki, Finland.

[s] Department of Stomatology, University de Montreal, Montreal, Canada, H3C 3J7.

Short Title: Oral Healing Between Mice and Axolotl

Corresponding Author:

*S.Roy & S.Tran. **S.R** @ U de M, 2900 Édouard-Montpetit, Montréal**,** P.O Box 6128 Station Centre-Ville, H3C 3J7, Tel: 514-343-6111 ext 1780; Fax: 514-343-2237. Email: stephane.roy@umontreal.ca, **S.T** @ McGill University, Faculty of Dentistry, 3640 University Street, Montreal, H3A 0C7, Tel: 514-398-7203; Fax: 514-398-8900. Email: simon.tran@mcgill.ca

Number of Tables: 0.

Number of Figures: 7.

Word count: Please indicate the word count including Abstract and body text. This is not to include the title page, reference list or figure legends.

Keywords: Please provide 3–5 keywords highlighting the most important points of your paper.

Abstract

The *Ambystoma maxicanum* (axolotl) regenerates strikingly from wounds and amputations. Comparing its healing ability to non-regenerative species such as the mouse, should help narrow in on mechanisms to improve human wound healing. Here, the tongue and intermandibular soft tissues of both mice (C57BL/6NCrl) and axolotls were wounded with a 2-2.5mm punch biopsy. The study aimed to resolve the differences between the two species; during surgical procedure, the macroscopic and histological characteristics. This including wound closure times, epithelial wound sealing and thickness as well as acute immune marker myeloperoxidase's (MPO) response over 30 days. Post surgery, mice visually showed greater haemorrhage; their wounds immediately collapsed while it took 14 days for the axolotls' mandibular void to close. The epithelium sealed the axolotls' wound margins within 24h with a maximal mean thickness of 0.42±0.13 fold normalized to unwounded skin. In mice, the epithelium separately sealed the ventral and dorsal sides, respectively at 7 and 7-30 days with mean maximal epithelial thicknesses reaching 13±5.6 and 3.0±0.63 fold. Mean MPO positive cell values peaked in axolotls at 14±1.5 fold between hours 6-12; while in mice, it peaked at 8.7±0.9 fold between hours 24-96. We conclude that axolotls form smaller blood clots, have a faster and thinner epithelial cell migrating front, and a shorter MPO positive cell response in comparison to mice. These observations may help refine future oral and facial wound healing research and treatment.

Introduction

Tissue regeneration in the craniofacial region is important, since a preference exists for an aesthetically pleasing, non-scarred appearance. Furthermore, several daily important tasks are performed by the lips, tongue, neck, chin and eyes; these include eating, breathing, speaking and vision.

In pursuit of finding alternatives to the current oral-maxillofacial surgical reconstruction standard, the tissue flap [Navarro Cuellaret al., 2015], we previously characterized the *Ambystoma mexicanum's* (axolotl) oral and neck tissue reconstruction/regenerative ability over 180 days [Charbonneauet al., 2016]. As an extension to this previous work, this current study compares the axolotl's wound healing to the corresponding wound in a mouse, a mammalian representative. Although the axolotl and mouse are both established as human models of research [Wonget al., 2011], direct comparative head and neck tissue wound healing studies are non-existent. The literature does provide some evidence of differences between healing, although not specifically related to the head and neck tissues. For instance, mice have greater haemorrhage and longer wound epithelial migration times [Seifertet al., 2012]. In this study, these aspects of wound healing are revisited.

Granulocytes are the first infiltrating immune cells in the wound, preventing infection and clearing damaged cells. Their infiltration and residency time in the wound are of importance as they can impact subsequent wound healing steps [Doviet al., 2004;Turabelidze and DiPietro, 2012]. A study found that axolotls had a weaker granulocytic response as compared to mice; unfortunately, quantitative data was absent [Seifertet al., 2012]. To fill this gap of information, a specific attention in this study is placed on the granulocyte profiles in the wounds. In non-comparative wound healing studies, the axolotl's granulocytic peak presence in the wound varies and has been identified at 48h [Levesqueet al., 2010], 72h [Seifertet al., 2012;Godwinet al., 2013] or 96h [Godwinet al., 2013]. For the sake of simplicity, more details on the immune response during tissue regeneration are summarized elsewhere [Godwin and Rosenthal, 2014;Godwinet al., 2017;Mescher, 2017;Mescheret al., 2017]. For the mammalian species, rodent wound healing, including experiments in rats [Bhaskar and Lilly, 1964;Standish and Eversole, 1970] and mice [Rovinet al., 1965;Doviet al., 2003;Kozlowskiet al., 2013;Pulliet al., 2013;Fuet al., 2014], a clearer consensus is noted; granulocyte infiltration commonly peaks near 24h post-injury. Subsequently, these cells remain on site for a few more days.

This exploratory study overviews the relatively early phases of wound healing including: haemorrhage/hemostasis [Oakley and Larjava, 2012], epithelial migration [Larjavaet al., 2012;Huanget al., 2017] and the inflammatory response [Turabelidze and DiPietro, 2012;Seifert and

Maden, 2014] after a similar wound in both animals' tongues and intermandibular regions. We expected the wounds to create observable and quantifiable data highlighting certain important differences in these animals early wound responses. To a certain extent, the data collected here can be extrapolated to humans and hypotheses made on novel oral-maxillofacial treatments inspired by the axolotls healing mechanisms.

The axolotl is our closest phylogenetic living relative able to regenerate the majority of its body parts. It is therefore important to identify —from macroscopic to microscopic— variations in cross species healing patterns.

Materials and Methods

Animal Surgeries and Maintenance

The details of the axolotl's (*A. mexicanum*) care have been previously described [Charbonneauet al., 2016]. Briefly, the axolotls were purchased from Ambystoma Genetic Stock Center (Lexington, KY) were fed with bloodworms and subjected 12h-12h light-dark cycle. Their containers were filled with 20°C Holtfreters 20% (v/v) and replaced every 2-3 days. As for the mice, briefly, they were kept in groups of six, in woodchips containing cages and fed with hard or water soften food. Animal care and procedures were approved and conducted in accordance to the guidelines provided by either: the Université de Montréal (for axolotls), the University of Oulu and the National Animal Experiment Board in Finland (ELLA, no: ESAVI/3739/04.10.07/2015) (for mice).

The axolotl oral-facial wounding was performed as described previously [Charbonneauet al., 2016]. Briefly, 8-10 cm long axolotls were anaesthetized (general) by immersion in 2X Ethyl 3-Aminobenzoate Methansulfonate or MS-222 (E10521, Sigma) and moved to a home-made plastic holding device. A metal spatula was inserted intra-orally on the top of the tongue and from the chin, a 2.5 mm punch biopsy resected intermandibular and tongue tissues. Without sutures or analgesics, the animal was reinserted in its liquid habitat for recovery. The axolotls' tissue processing into paraffin blocks were performed as described [Charbonneauet al., 2016]. In total, 4-axolotls/time point were examined. Male C57BL/6NCrl (Charles River, www.criver.com) 4-5 months old mice, were administered anaesthetic cocktail [Ketamine 75mg/kg (Ketaminol, Intervet), Xylazine 10mg/kg (Rompun, Oriola) and Acepromazine 3mg/kg (Plegicil, Oriola,)] subcutaneously. While anaesthetized, the mice received Oftagel (Santen) to moisten their eyes, their wounding site shaved and wiped with sterile water. Similar to the axolotl, an in house reusable plastic holding device was used to assist the procedure (Fig. 1A, Sup. Info 1). While the mouth was maintained open and the tongue slightly pulled out with two metal tweezers, a metal spatula was inserted deep into the mouth. Then, starting from

the chin, a 2mm punch biopsy resected intermandibular and tongue tissues. A 2mm biopsy was used since the intermaxillary region could not host larger. Without pressure or stitching to the wound, a prompt suctioning of blood —with a syringe linked to a protective sleeve of a Venflon Pro IV Catheter (393204, BD Scientific)— was used when needed, to prevent haemorrhage-induced suffocation. An anaesthetic antidote Antipamezole 1mg/kg (Antisedan, Orion) and physiological saline solution (0.5mL) were separately injected subcutaneously right after wounding and the mice were moved to 37°C for three days. For the same period of time they received analgesics 0.1mg/kg buprenorphine (Vetergesic, Orion) every 8-12h. After CO_2 euthanasia, the mice's lower jaws were isolated with scissors.

Histology and immunohistochemistry

The handling of axolotls histological samples has been previously described (2). Mouse tissues were soaked in 10% formalin for 24-48h and rinsed with running tap water for several hours. The mouse samples were decalcified for 12-21 days in 0.5M ETDA at pH 7.4 with heating and stirring at 37°C in a Multifunctional Microwave Histoprocessor (T/T MEGA, Milestone). Mouse samples were vacuum embedded in paraffin (Tissue Tek VIP 5 Jr, Sakura), serially sectioned at 8µm between both rows of molars and every 10^{th} section mounted. On average 3.3-mice/time point were examined. Tissue sections on glass slides were rehydrated to water; then soaked for 10min in both Mayer's Hematoxylin (MHS1, Sigma), then Eosin Y (HT110232, Sigma), dehydrated and mounted. To stain for myeloperoxidase (MPO), all tissue sections were rehydrated and heated to near 100°C for epitope retrieval in glass Coplin jars in Citrate Buffer pH 6 (S2031, Dako) for 20min. After cooling, the samples were incubated with first peroxidase blocking solution (S202386, Dako) and then 5% Blotting Grade Blocker (170-6464, BIO RAD) for 5 and 10 min. Subsequently, the MPO antibody (RB-373-AO, Thermo Fisher) at a dilution of 1:100 or negative control —non-immunized rabbit serum (X0903, Dako) — were added and the slides were placed in a humid chamber at 4°C overnight. The following day the HRP linked secondary antibody (K5007, Dako) was also added for 30min. Afterwards, specific chromogens were applied to each species. The axolotl samples were first counter stained with Kernechtrot (0.1g (nuclear Fast Red, C.I 60860) in 100mL of 5% Aluminum Sulfate X $18H_20$, heated, cooled down and filtered) for 5 min and rinsed in running water for 3min. Then the TMB chromogen (SK-4400, Vector Lab Inc.) was added for 1-2mins followed by a rapid water rinse and dehydration with hotplate. Mouse samples were first stained with DAB chromogen (K5007, DAKO) for 45s, counter stained with Myers Hematoxylin for <7min and nuclei blued in 0.03% ammonium water. All slides were mounted with a coverslip and organic medium.

Imaging

Macroscopic axolotl images were taken with MZ16F stereomicroscope (Leica); mice images with iPhone 4s. Histology slides were scanned with an Aperio AT2 Automated Slide Scanner (Leica).

Microscopy Quantification

All epithelial gap and epithelial thickness measurements were conducted on scanned slides with software ScanScope 12.4 (Leica). Measurement examples are found in Sup. Fig. 1. The measurement values were then converted to fold measurements by normalizing the values to baseline. Briefly, the axolotls' gap was measured on the posterior side of the wound. The digital ruler spanned the wound margins from the ventral (skin) to the dorsal (tongue) side. For the mice, two wound measurements were taken; the digital ruler always spanned between anterior to posterior epithelial wound margins on the ventral and dorsal gaps. Epithelial thickness was based on the average of two measurements taken from each extremity of the gap measurement.

To count MPO-positive nuclei in axolotls, 3-6 serial sagittal section images from each animal were manually blindly analyzed. The serial sections included the middle and lateral sides of the wound as well as a negative control taken >10mm away from the wound's margins. In mice, MPO quantities were taken from the average of two sagittal sections images obtained between rows of molars. Counted by automation, the quantification area is described in Sup. Fig. 2 and the algorithm from Volocity 5.4.1 (Perkin Elmer) is described in Sup. Info 2. Positive cells found at T=0 were subtracted as false positives.

Statistical Analysis

Interspecies and time epithelial gap percentages to closure, epithelial thicknesses fold increase and MPO^+ cell fold increase counts were statistically analyzed by two way ANOVA using Graphpad Prism 7 software. Significance was achieved when $p=\leq 0.05$.

Results

Various differences between the species were observed in the wounded tissue area.

The wounding set-up is illustrated with pictures (Fig. 1A and J). Furthermore, histologically stained lower jaw sagittal sections are shown to demonstrate each animal's unwounded wounding site (Fig. 1G and K). At the wounding locations, the mice's sagittal sections contained mostly muscle (Fig. 1G). In the axolotl, aside from muscle, there was a hyoid arch cartilage and more connective tissue (Fig. 1K). In blood vessels, the axolotl's mostly nucleated cells contrasted with the mouse's lesser-nucleated blood cells (Figs. 1H, I). Axolotls' hairless and translucent skin perceptively felt easier to wound and more fused with the deeper tissues (Fig. 1C, E vs. Fig. 1M, O). The axolotl had a larger oral

maximal opening in the horizontal and vertical directions, but mice tongues had greater degrees of freedom for movement.

Macroscopically, the mouse's wound collapses and fills with a clot contrasting the axolotl's low haemorrhage and open wound healing sequence.

Surgical survival rates for both species approached ~85%. The body weights decreased temporally after wounding, improving after 1 and 3 days for axolotls and mice, respectively (Sup. Fig. 3). Initially, both chin wounds caused cylindrical gaps in the lower jaws (Fig. 2B, D). In mice, the ventral visibility into the wound was quickly concealed by looser skin and bleeding (Fig.2B). In axolotl, a clear visual view of the semicircular exiting tongue wound was maintained over time (Fig. 2D). With its small oral opening, mice's dorsal tongue wounds could only be evaluated after euthanasia and surgical mandibular maxillary separation (Fig. 2A). After 12 hours, the mice's chin wounds possessed a protruding scab while the axolotl's wound remained unobstructed and open (Figs. 2F. vs. 2H). The mice remained immobile while the axolotls were swimming but seemed less stimulated by food. At 24 hours, mice began walking but advanced slowly. Externally on certain mice's chins, the scab had disappeared, and a dark red clot was observed containing bright spots (Fig. 2J). In the mice's oral cavity, instead of a clot, a discolouration of the tongue's tissue near the exiting wound was noticed (Fig. 2I). As for the axolotl, we previously described the wound healing observations in detail [Charbonneauet al., 2016]. Important for the future discussion though is a yellow mass outlining the internal surfaces of the axolotl's wound (Fig. 2L). After 48h on the mice's chins, flush with the skin and over the clot, a conspicuous yellow layer was also noted (Fig. 2N). At 96h, the mice's behaviours had returned to normal. From 96h to 7d mice's hairs grew proximally to the wound's margins, concealing its outline (Fig. 2R). In some mice autopsies, a yellow layer was observed on exiting tongue wounds as well (Fig. 2Q). In the axolotl's, some tissue buds progressed equally from the margins until chin wound closure at 14 days (Fig. 2T). After 30 days, the axolotls' tongues were not yet symmetrical to the unwounded sides (see other publication [Charbonneauet al., 2016]. In mice, from 7 to 30 days, —because of hair and small oral opening—their ventral and dorsal wound's location remained a challenge to visualize.

The axolotl's migrating epithelium is thinner and seals the wound faster.

Immediately after injury, the sagittal sections of both animals had a tissue void (Fig. 3A, B, C). The axolotls' baseline mean unwounded epithelia were 49.3µm±13.6 on the ventral and dorsal sides. Respectively, for mice, baseline values were 10.4µm±1.28 and 50.5µm±13.8 (Fig. 4A, B, C). At 12h, the axolotl's migrating epithelial was on average thinner than baseline (0.62 fold ±0.26). Importantly, within 24h, the migrating epithelium had completed a 100% dorsal-ventral migration on both the

anterior and posterior vertical walls of the wound (Fig. 3G, M); its thickness measured on average 0.42 fold±0.13 (Fig. 4M). At 24h, between species, there was a significant difference in epithelial wound closure. In axolotls, —without rapid antero-posterior wound closure by a clot or contraction (as seen with the mice) —, it was in this vertical direction that the axolotls epithelium first migrated. Antero-posterior epithelial thickening was observed but only once the epithelial cells had thinly sealed the wound margins. Over 7 days though, the axolotls' overall general epithelial thickness (excluding larger cell masses) never thickened enough to reach statistical significance (Fig. 4J, M). In mice, within the first 24h, the ventral and dorsal epithelium gap —seen on sagittal sections— had, respectively, 83%±14 and 69%±39 remaining distance to close (Fig. 3E, F, M). Epithelial cells had not yet started their migration (Fig. 4E) on the ventral and dorsal sides (Fig. 4F). Importantly —in contrast to the axolotls— the mice's epithelial cells migrated horizontally in an anterior-posterior direction. The cell migration started only after epithelial thickening. Beyond 48h, the mean ventral epithelial gap percentage to closure was 55%±15 (48h), 32%±15 (4d), 4.9%±4.2 (7d) (Fig. 3M). At these respective times, the ventral wound's margins epithelial thickness increased (3.07±0.85, 4.19±1.7, 13.1±5.6) (Fig. 4M). After 7d, epithelium sealed the entire ventral gap in most animals (Fig. 3K, M), the percentage to closure was also significantly different than the dorsal gap. The mean percentages to closure on the dorsal side were 47%±12 (48h), 42%±16 (4d) and 55%±14 (7d) (Fig. 3L, M). Over time the dorsal wounds epithelial fold thickness was 1.18±0.14(48h), 2.01±0.52(4d), 2.99±0.63 (7d). The ventral epithelium had a significantly greater fold increase in thickness compared to the dorsal side only as of the 7th day (Fig. 4L, M). The dorsal gap on the mouse was sealed last between the 7th and the 30th day. After 30 days, histologic analysis of both species demonstrated a trajectory of cellular disorganization within the tongue's muscle (Sup. Fig. 4). In both species, the skin looked relatively normal and the transverse subcutaneous muscle had returned. On histology sections of both species tongues, a visible ventral-dorsal pit lingered (Sup. Fig. 4). In two separate mouse sections, a salivary gland infection and foreign body encapsulation were observed (Sup. Fig. 5A-D); interestingly, the histology of axolotl tissues never revealed such surgically induced side effects.

Axolotls' relatively higher peaking MPO positive cells appeared earlier, but resided in the wound for a shorter period of time.

In almost all axolotl MPO stained sagittal sections, positive cells were found within 12h, posterior to the wound and within the connective tissue and the deteriorating muscle (Fig. 5B, C). In mice at 12h few MPO positive cells were detected (Fig. 6A). For the amphibian MPO containing cells, quantities peaked at the 6th and the 12th hour post surgery with values representing a mean fold increase of 7.6±0.9 and 13±0.7 respectively compared to the baseline (unwounded, 5.41cells±5.7).

The peak fold increase at the 6th and 12th hour significantly differed ($p<0.05$) compared to the baseline and all other times (0.7±0.2 (24h), 1.1±0.6 (48h), 2.7±0.7 (4d), 1.45±0.4 (7d)) (Fig. 7). For mice, the peak came later were mean MPO fold increased reached 6.1±0.7 (24h), 7.9±1.2 (48h), 8.7±0.9 (4d) compared to the baseline (unwounded, 1.31Kcells±544) and infiltrated the wound's muscle, fat, or connective tissue (Fig. 6B, C). These values were significantly greater ($p<0.05$) than the baseline and other time points (3.9±0.6 (12h), 3.5±1.4 (7d) (Fig. 7).

Discussion/Conclusion

This exploratory study was designed to identify highly contrasting events in the wound-healing sequences of regenerative axolotl and non-regenerative mouse. Importantly, the mice's wounds contract faster and have larger haemorrhages and clots. Furthermore, the axolotls had a thinner epithelial bud thickness, faster epithelial migrating speeds as well as a shorter MPO positive cell presence in the wound.

In terms of oral-maxillofacial comparative anatomy, the axolotl's "tongue" —as we referred in this study— is not exactly a tongue in the mouse or human's sense. Rather, the axolotl's wounded tissue relates to a more posterior structure than a "tongue". This is exemplified by the hyoid arch in the axolotl's "tongue". The axolotl develops a true "tongue" only through induced metamorphosis [Grevenet al., 2013;Ziermann and Diogo, 2013]. This could explain the difference in muscle and cartilage. Furthermore, the tongues' degrees of freedom result from their attachment points —wide in the axolotl and thin in mice— and tissue composition (all muscle vs. muscle and cartilage). Sagittal section of the blood vessels showed larger nucleated cells in the axolotl. This is in-line with others who have shown other amphibians possess nucleated erythrocytes with a larger mean corpuscular volume compared to humans [Lewis, 1996;Lopezet al., 2014].

The mice's rapid skin contraction was most likely caused by the subcutaneous panniculosis carnosus muscle [Sundbergt al., 2018]. Furthermore, mice are known to have loose-skin contrasting the tight-skinned axolotls and humans [Denisel al., 2013]. Even though the axolotl's wound remains open, this specie has relatively less haemorrhage. Seifert et al. also observed greater hemostasis in axolotl compared to mice[Seifertet al., 2012]. Haemorrhage has been reported in amphibians [Tanket al., 1976] and salamanders [Younget al., 1983b] but our observations specifically use comparative wound healing to discuss relative haemorrhage. Interestingly, lower vertebrates such as birds, fish, certain amphibians and reptiles possess thrombocytes, a specialized nucleated cell akin to the mammalian platelet [Emmel, 1925;Belamarich, 1976]. In axolotl, investigating this cell's role in early

wound healing and regeneration would be beneficial. In other studies, only the urodele, not anuran amphibian coagulation times were slightly faster than in humans [Lewis, 1996] suggesting that urodele amphibians possess a more favourable coagulation mechanism. The reduced haemorrhage could also be as a result of the axolotl's more lateral wounding location (Sup. Fig. 5E), less muscle in the wound's trajectory, the avoidance of certain blood vessels identifying anatomical landmarks, the animals' weights, blood pressure or metabolism (ex: endothermic).

The absence of substantial haemorrhage and clot in the axolotl's wound appears to contribute to the more efficient wound epithelialization. Similar to the void in this oral wound, other amphibian wound healing studies also suggest the importance of a void. For instance, obstructions such as skin grafts placed over an amputated limb, prevent its regeneration [Tassava and Garling, 1979]. Furthermore, in regenerating amphibians studies, the literature never describes granulation tissue, the substance that fills mammalian wound voids; rather, a blastema forms[Tanaka and Reddien, 2011]. This organization centre for regeneration migrates into a void, not into a clot. Future comparative wound healing studies should consider defining differences between early amphibian blastema components and mammalian granulation tissue. The mice's relative reduced re-epithelization rates and absence of blastema formation may in part be due to obstruction by a clot and granulation tissue that fills the void. The presence of the clot and contraction could explain the mouse's larger epithelial front. A larger mass of cells permits the production of more enzymes needed to degrade the damaged contracted tissue and clot [Larjavaet al., 2012]. The axolotl's liquid environments may alter the blood clot's formation contrasting open-air wounds. Similarly in humans', improved wound healing occurs in two documented situations involving liquids: in the womb during fetal development [Lorenzet al., 1992;Kawasumiet al., 2013] or inside the oral cavity [Szpaderskaet al., 2003;Turabelidze and DiPietro, 2012]. These interesting liquid environment similarities are certainly not the only factor permitting regeneration. For instance, certain terrestrial salamanders regenerate [Ferretti, 1996] although slower [Younget al., 1983a] and other aquatic amphibians do not regenerate (necturus and frogs).

In this study, the acute inflammation was estimated as the number of MPO^+ cells. Although MPO^+ cells' fold increase was used as one of the parameters to compare both species responses, the different baseline cell densities must be kept in consideration; generally speaking, the mouse tissues we examined had substantially greater cell densities. With such a cell density discrepancy, we place more "weight" of the evidence on the time MPO^+ cells' remained in the wound. The shorter MPO presence in axolotl can be explained by the absence of a clot that would usually —through its chemotactic properties [Häkkinenet al., 2012]— attract inflammatory cells. In the same manner, the

mouse's clot's chemotactic properties may maintain mouse MPO positive cells in proximity to the wound. Interestingly, both axolotls and mice MPO levels followed a trend. The decrease in MPO levels coincides with the sealing of the wound by the epithelial cells. Accordingly, there may be in this process, an underlying communication between epithelial cells' coverage of the wound and MPO^+ cells counts. Overall, the results clearly demonstrate axolotl's earlier and shorter MPO^+ cell response.

In our previous study [Charbonneauet al., 2016], we set a particular attention on a visible yellow mass observed in the axolotls' wounds. Its macroscopic location matched the location of epithelial keratinocytes identified by immunofluorescence staining. Now we also observed this macroscopic yellow substance in mice 48h post surgery. At 48h, the epithelial cells have not yet sealed the wound. This suggests that the yellow substance might not originate from the accumulation of epithelial cells. Rather, it may originate from an extracellular protein used by both species wound healing process.

Despite the anatomical, metabolic and habitat differences between species, we felt wound healing data was lacking from the perspective of a direct comparison between axolotls and mice. We did not observe important histologic contrasts between the animals at 30 days. Others have reported impressive healing in mammals after full thickness excisional wounds; accordingly, this mice strain may possess a special healing potential[Seifert and Maden, 2014]. The fact remains that we still note a few important points that contrast their healing patterns: Axolotls don't form as large clots; they have a faster and thinner epithelial migrating front and an earlier and shorter MPO^+ cell response in comparison to mice. We encourage others to build on this preliminary work to suggest more mechanisms on the axolotl's outstanding regenerative ability and bring human's tissue regeneration within closer reach.

Statements

Acknowledgement (optional)

We thank Dr. Antonio Nanci and his team for lending tissue processing and imaging equipment for most of the axolotl's histological samples. Additionally, enormous gratitude is forwarded to the Department of Pathology at the University of Oulu for the lending of their automated machines contributing to the processing, staining and digitization of sagittal sections in mouse and axolotl. Special thanks to Michael Smith and the contributors to his legacy scholarship fund that allows Canadian students to work abroad and have international research experience.

Statement of Ethics

Conflict of Interest Statement

The authors declare no conflict of interest.

Funding Sources

Canadian Institutes of Health Research (CIHR-81381) and the Réseau de Recherche en Santé Buccodentaire et Osseuse (RSBO-233425) (**SR** and **ST)**. CIHR scholarships CGS-M and Michael Smith Foreign Study Supplement, McGill University Faculty of Dentistry, Saputo Family, Mrs. Pierrette Wong, the Dairy Farms of Canada and the Network for Canadian Oral Health Research (NCOHR) (**AMC**). The Sigrid Juselius Foundation and MRC Oulu University Hospital grant (**TS**)

Author Contributions

[AC] designed, conducted all experiments and obtained certain funds. [PÅ] contributed to the experimental design and mice experiments and proofread the manuscript. [TS, SR, ST] contributed funding, equipment and proofread the manuscript. [SR and ST] also contributed to the axolotls' wound design.

References [Alphabetical]

Belamarich FA. Hemostasis in animals other than mammals: the role of cells. Prog Hemost Thromb. 1976;3:191-209.

Bhaskar SN, Lilly GE. Traumatic Granuloma of the Tongue (Human and Experimental). Oral Surg Oral Med Oral Pathol. 1964 Aug;18:206-18.

Charbonneau AM, Roy S, Tran SD. Oral-Facial Tissue Reconstruction in the Regenerative Axolotl. J Exp Zool Part B Mol Dev Evol. 2016;326(8):489-502.

Denis J-F, Lévesque M, Tran SD, Camarda A-J, Roy S. Axolotl as a Model to Study Scarless Wound Healing in Vertebrates: Role of the Transforming Growth Factor Beta Signaling Pathway. Adv Wound Care. 2013 11/30/received;2(5):250-60.

Dovi JV, He L-K, DiPietro LA. Accelerated wound closure in neutrophil-depleted mice. J Leukocyte Biol. 2003 April 1, 2003;73(4):448-55.

Dovi JV, Szpaderska AM, DiPietro LA. Neutrophil function in the healing wound: adding insult to injury? Thromb Haemost. 2004;92(2):275-80.

Emmel VE. Studies on the non-nucleated cytoplasmic elements of the blood. III. Leucoplastids or non-nucleated leucocytic derivatives in vertebrates other than mammals. Am J Anat. 1925;35(1):31-61.

Ferretti P. Re-examining jaw regeneration in urodeles: what have we learnt? Int J Dev Biol. 1996 Aug;40(4):807-11.

Fu Y, Zhou E, Wei Z, Liang D, Wang W, Wang T, et al. Glycyrrhizin inhibits the inflammatory response in mouse mammary epithelial cells and a mouse mastitis model. FEBS J. 2014;281(11):2543-57.

Godwin JW, Pinto AR, Rosenthal NA. Macrophages are required for adult salamander limb regeneration. Proc Natl Acad Sci U S A. 2013 June 4, 2013;110(23):9415-20.

Godwin JW, Pinto AR, Rosenthal NA. Chasing the recipe for a pro-regenerative immune system. Semin Cell Dev Biol. 2017 1//;61:71-79.

Godwin JW, Rosenthal N. Scar-free wound healing and regeneration in amphibians: Immunological influences on regenerative success. Differentiation. 2014 1//;87(1–2):66-75.

Greven H, Richter H, Clemen G. Formation of the secondary tongue in Hynobius leechi and Ambystoma mexicanum (Amphibia: Urodela). VERTEBRATE ZOOLOGY. 2013;63(2):217-32.

Häkkinen L, Larjava H, Koivisto L. Granulation Tissue Formation and Remodeling. Oral Wound Healing. John Wiley & Sons, Ltd.; 2012. p. 125-73.

Huang T-Y, Chang C-C, Cheng N-C, Wang M-H, Chiou L-L, Lee K-L, et al. Re-epithelialization of large wound in paedomorphic and metamorphic axolotls. J Morphol. 2017;278(2):228-35.

Kawasumi A, Sagawa N, Hayashi S, Yokoyama H, Tamura K. Wound Healing in Mammals and Amphibians: Toward Limb Regeneration in Mammals. In: Heber-Katz E, Stocum DL, editors. New Perspectives in Regeneration. Berlin, Heidelberg: Springer Berlin Heidelberg; 2013. p. 33-49.

Kozlowski C, Jeet S, Beyer J, Guerrero S, Lesch J, Wang X, et al. An entirely automated method to score DSS-induced colitis in mice by digital image analysis of pathology slides. Disease Models & Mechanisms. 2013;6(3):855-65.

Larjava H, Häkkinen L, Koivisto L. Re-Epithelialization of Wounds. In: Larjava H, editor. Oral Wound Healing. John Wiley & Sons, Ltd.; 2012. p. 81-123.

Levesque M, Villiard E, Roy S. Skin wound healing in axolotls: a scarless process. J Exp Zool B Mol Dev Evol. 2010 Dec 15;314(8):684-97.

Lewis JH. The Amphibians. Comparative Hemostasis in Vertebrates. Boston, MA: Springer US; 1996. p. 71-84.

Lopez D, Lin L, Monaghan JR, Cogle CR, Bova FJ, Maden M, et al. Mapping hematopoiesis in a fully regenerative vertebrate: the axolotl. Blood. 2014;124(8):1232-41.

Lorenz HP, Longaker MT, Perkocha LA, Jennings RW, Harrison MR, Adzick NS. Scarless wound repair: a human fetal skin model. Development. 1992 Jan;114(1):253-9.
Mescher AL. Macrophages and fibroblasts during inflammation and tissue repair in models of organ regeneration. Regeneration (Oxf). 2017 Apr;4(2):39-53.
Mescher AL, Neff AW, King MW. Inflammation and immunity in organ regeneration. Dev Comp Immunol. 2017 1//;66:98-110.
Navarro Cuellar I, González Otero T, Ruiz Cruz JA, Navarro Vila C. Reconstruction of Soft Tissue Defects Using Microsurgical Flaps. Cham: Springer International Publishing; 2015.
Oakley C, Larjava H. Hemostasis, Coagulation and Complications. In: Larjava H, editor. Oral Wound Healing. Chichester, West Sussex: John Wiley & Sons; 2012. p. 11-38.
Pulli B, Ali M, Forghani R, Schob S, Hsieh KL, Wojtkiewicz G, et al. Measuring myeloperoxidase activity in biological samples. PLoS One. 2013;8(7):e67976.
Rovin S, Costich ER, Fleming JE, Gordon HA. Healing of Tongue Wounds in Germfree and Conventional Mice. Arch Pathol. 1965 Jun;79:641-3.
Seifert AW, Maden M. Chapter Four - New Insights into Vertebrate Skin Regeneration. In: Jeon KW, editor. Int Rev Cell Mol Biol. Academic Press; 2014. p. 129-69.
Seifert AW, Monaghan JR, Voss SR, Maden M. Skin Regeneration in Adult Axolotls: A Blueprint for Scar-Free Healing in Vertebrates. PLoS One. 2012;7(4):e32875.
Standish SM, Eversole LR. Regenerative changes in rat tongue muscle following crushing injury. Oral Surg Oral Med Oral Pathol. 1970 Jul;30(1):87-98.
Sundberg JP, Booth CJ, Nanney LB, Fleckman P, King LE. 24 - Skin and Adnexa. In: Treuting PM, Dintzis SM, Montine KS, editors. Comparative Anatomy and Histology (Second Edition). San Diego: Academic Press; 2018. p. 511-42.
Szpaderska AM, Zuckerman JD, DiPietro LA. Differential injury responses in oral mucosal and cutaneous wounds. J Dent Res. 2003 Aug;82(8):621-6.
Tanaka Elly M, Reddien Peter W. The Cellular Basis for Animal Regeneration. Dev Cell. 2011;21(1):172-85.
Tank PW, Carlson BM, Connelly TG. A staging system for forelimb regeneration in the axolotl, Ambystoma mexicanum. J Morphol. 1976 Sep;150(1):117-28.
Tassava RA, Garling DJ. Regenerative responses in larval axolotl limbs with skin grafts over the amputation surface. J Exp Zool. 1979 Apr;208(1):97-110.
Turabelidze A, DiPietro L. Inflammation and Wound Healing. In: Larjava H, editor. Oral Wound Healing. Chichester, West Sussex: John Wiley & Sons; 2012. p. 41-42,48.
Wong VW, Sorkin M, Glotzbach JP, Longaker MT, Gurtner GC. Surgical Approaches to Create Murine Models of Human Wound Healing. 2011.
Young HE, Bailey CF, Dalley BK. Environmental conditions prerequisite for complete limb regeneration in the postmetamorphic adult land-phase salamander, Ambystoma. Anat Rec. 1983a Jul;206(3):289-94.
Young HE, Bailey CF, Dalley BK. Gross morphological analysis of limb regeneration in postmetamorphic adult Ambystoma. Anat Rec. 1983b Jul;206(3):295-306.
Ziermann JM, Diogo R. Cranial Muscle Development in the Model Organism Ambystoma mexicanum: Implications for Tetrapod and Vertebrate Comparative and Evolutionary Morphology and Notes on Ontogeny and Phylogeny. Anat Rec. 2013;296(7):1031-48.

Figure Legends

Figure 1: Surgical, macroscopic and microscopic differences between unwounded species. A,J) Animal wounding procedures. B-E, L-O) Animals' unwounded chin and tongue. Black and white boxes are higher magnification. The tongue images were captured after mandibular and maxillary separation. F,P) Simplified sketch of animals anatomies and wounding trajectories (dotted line). G,K) Sagittal sections of lower jaws in both species stained with hematoxylin and eosin. The full purple lined box on sagittal sections represents approximate wounding trajectory. H,I) Higher magnification of both species blood vessels. Abbreviations: muscle ligualis proprius (mus. l.p), muscle panniculus carnosus (mus. p.c), muscle genioglossus (mus. g), salivary gland (Sal.gland), muscle brachiohyoideus (mus. b.h.), muscle intermandibularis Posterior (mus. i.p.), hyoid arch (Hy. arch).

Figure 2: Key macroscopic images of the wounds in both species over 7 days. The yellow dots in certain mouse images are reference points (similar to a crosshairs) to help identify — when it is less obvious — the wound locations. Column 1 shows the wound on the mice tongues. Column 2 shows the wound on the mice chins. Column 3 shows the wound on the axolotls tongues. Column 4 shows the wound on the axolotls chins. W= Woodchips, scab now gone. Row 5,6,7: Yel= Yellow mass of cells. All scale bars = 1mm.

Figure 3: **H&E stained sagittal sections of the animals' wounds digitized to show remaining wound gap distance over 7 days.** The black arrowheads indicate epithelial margin locations. Furthermore, the blue arrowhead indicates when contact occurs between epithelial margins. A,D,G,J) Axolotls' dorsal and ventral wound healing at 4 time points over 48h. Sagittal section show: A) the fresh wound, D) the thin migrating epithelium, G) the wound sealed by the epithelium, J) the thickening of the epithelium. B,E,H,K) Mice wound sagittal sections focusing on the ventral chin at 4 time points

over 7d. B,E) No epithelial migration was observed. H) epithelial migration, K) completion of migration after 7d. C,F,I,L) Mice ventral wound (tongue) sagittal sections. C,F) The epithelium is still at the wounds margins. I,L) Epithelium is migrating to close the wound. M) Quantification of the distance remaining between epithelial wound margins. Scale bars all = 0.5mm. Error bars=SD. n = 2-4. *p-value≤0.05.

Figure 4: H&E stained sagittal sections of the animals' wounds digitized to show epithelial margin thicknesses over 7 days. Large single black arrowheads indicate epithelial margins. Small black triple arrowheads indicate projected direction of migration. A,D,G,J) Axolotls epithelial migration imaged at 4 time points over 48h. A) Epithelial edge of the fresh wound. D) Migrating single layer epithelium. G) A single layer of cells is contacting between dorsal and ventral sides. J) Thickening of the joined epithelium. B,C,E,F,H,I,K,L) Mice ventral and dorsal epithelial migration imaged at 4 time point over 4d. B,C) Epithelial edge of the fresh wound. E,F,H,I) Still no significant thickening. K,L) Thicker appearing epithelium but still not significant. M) Quantification of the epithelium margin thicknesses over 7d. All Scale Bars = 100um. Error bars = SD. n-value = 2-4. *p-value≤0.05.

Figure 5: Axolotl sagittal sections stained by immunohistochemistry demonstrating MPO positive cell distribution and appearance over time. Counterstain is red while positive signal is blue. The larger panels show the entire sagittal section of the lower jaw. In those panels, smaller numbered boxes (SB) identified the location of the magnified images. A) 30min post surgery. SB show nuclei in connective tissue (A1, A2) and near some muscle (A3, A4). Panel B) 6 hours post surgery. SB shows positive cells (arrowhead). Panel C) 12 hours post surgery. SB shows mostly cells in connective tissue with positive cells (arrowhead) still present. Panel D) 24h post surgery. SB shows a seemingly increase in cell numbers but decrease in MPO signal.

Figure 6: Mouse sagittal sections stained by immunohistochemistry demonstrating MPO positive cell distribution and appearance over time. Counterstain is shades of blue while positive signal is intense brown. At each time point, the larger sagittal section panels show a part of the lower jaw. In those panels, small numbered boxes identify the location of the magnifications. A) Fresh wound post surgery with a large gap between anterior and posterior sides of the wound. A123 No true positive signal in muscle, fat or connective tissue. B) 24 hours post surgery. The skin layer and underlying deeper tissue visually seemed disturbed. B123, There was localized dark brown MPO^+ signal near nuclei of certain cells. C) 4 days post surgery. Apparent MPO^+ positive signals and visual defects in the tissue are seen in the wound. C123 showed very dark brown signal near nuclei of certain cells. D) 7 days post surgery. In the skin and tongue side, tissue architecture appears disturbed. D123, showed cellular disorganization, an increased cell population with less dark brown signal.

Figure 7: Quantitative analysis of MPO^+ cells in the axolotls and mice over time. A) The data was obtained from counting MPO^+ cells in histological sagittal sections near the wound. Sup. Fig. 1 shows the approximate distance from the wound at which the tissues analysis in mice began; in the axolotl, there was no distance limit. The symbols indicate the mean±SEM. The quantity of animals and sagittal sections analyzed are also displayed below the graph. *p-value≤0.05.

Figure 1

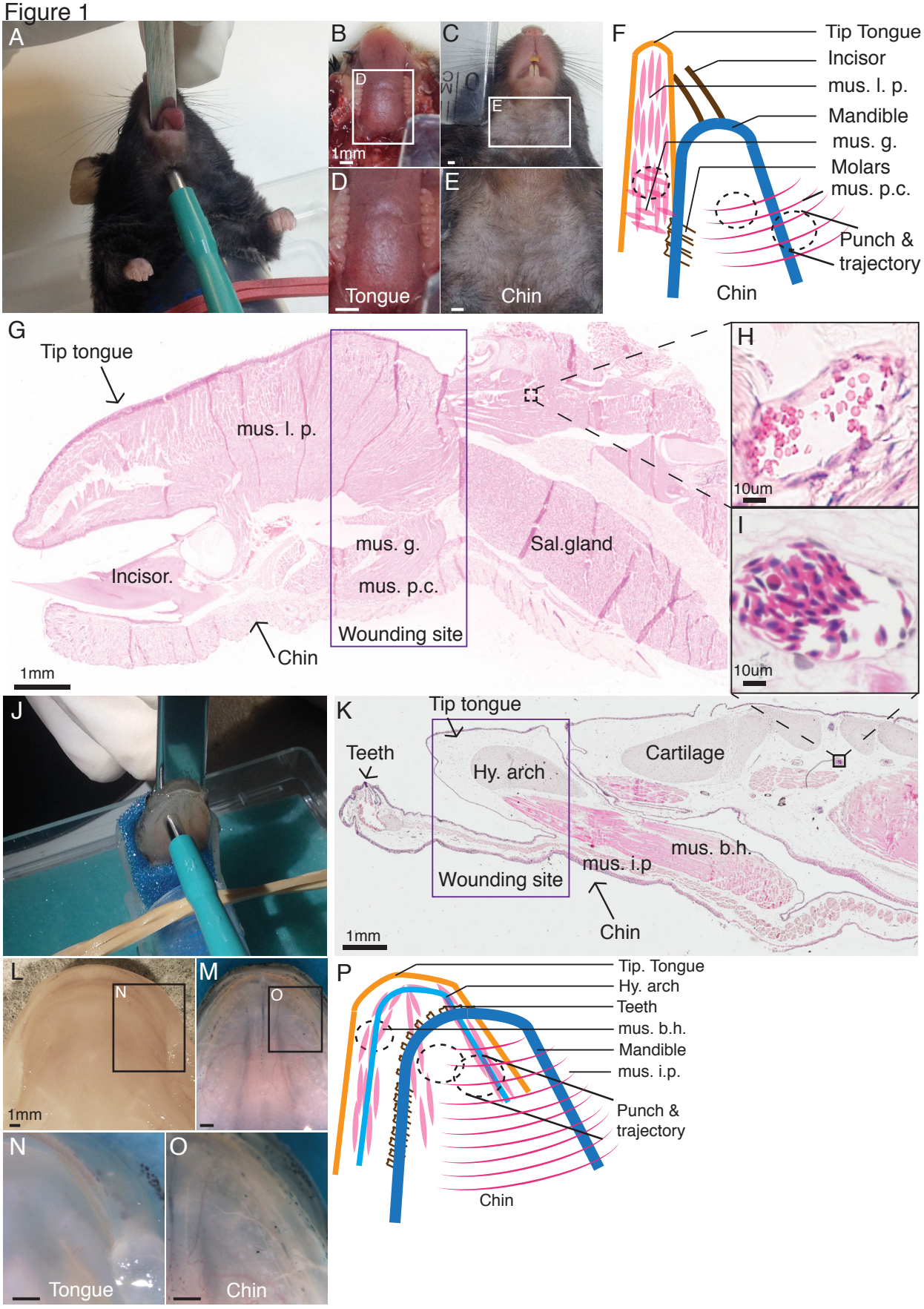
A
B
C
D
E
1mm
Tongue
Chin
F
Tip Tongue
Incisor
mus. l. p.
Mandible
mus. g.
Molars
mus. p.c.
Punch &
trajectory
Chin
G
Tip tongue
mus. l. p.
mus. g.
mus. p.c.
Wounding site
Sal.gland
Incisor.
Chin
1mm
H
10um
I
10um
J
K
Tip tongue
Teeth
Hy. arch
Cartilage
mus. b.h.
mus. i.p
Wounding site
Chin
1mm
L
M
N
O
1mm
N
O
Tongue
Chin
P
Tip. Tongue
Hy. arch
Teeth
mus. b.h.
Mandible
mus. i.p.
Punch &
trajectory
Chin

Figure 2


Mouse
Axolotl
T=0
T=12h
T=24h
T=48h
T=7d
A
B
Abundant Bleeding
C
D
Minimal Bleeding
1mm
E
F
Visible Clot
G
H
No Visible Clot
I
J
W.
K
Yel.
L
Yel.
M
N
Yel.
O
P
Yel.
Q
Yel.
R
S
T

Figure 3

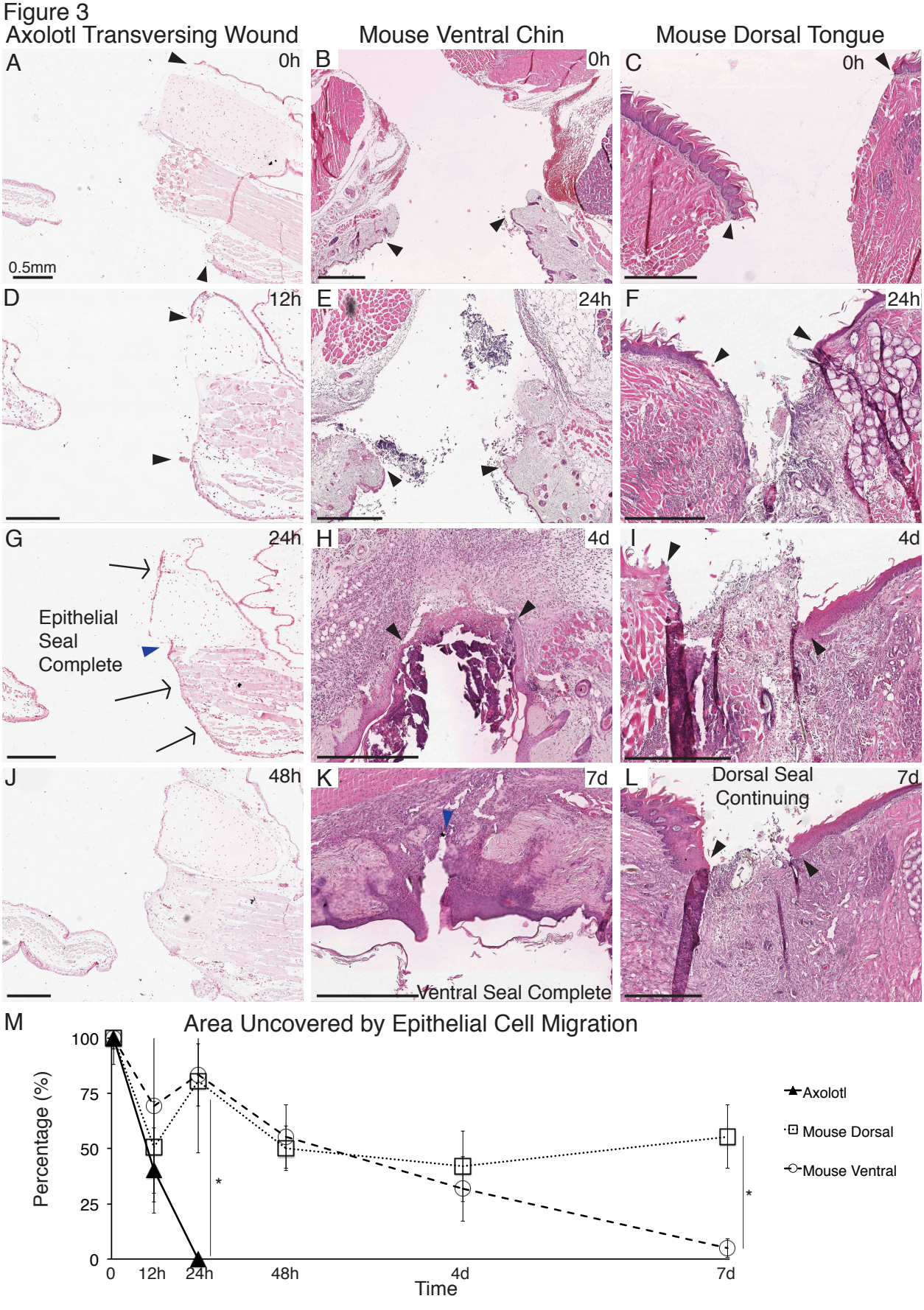
Axolotl Transversing Wound
Mouse Ventral Chin
Mouse Dorsal Tongue
A
0h
0.5mm
B
0h
C
0h
D
12h
E
24h
F
24h
G
24h
Epithelial
Seal
Complete
H
4d
I
4d
J
48h
K
7d
Ventral Seal Complete
L
Dorsal Seal
Continuing
7d
M
Area Uncovered by Epithelial Cell Migration
Percentage (%)
100
75
50
25
0
0
12h
24h
48h
4d
7d
Time
*
*
Axolotl
Mouse Dorsal
Mouse Ventral

Figure 4

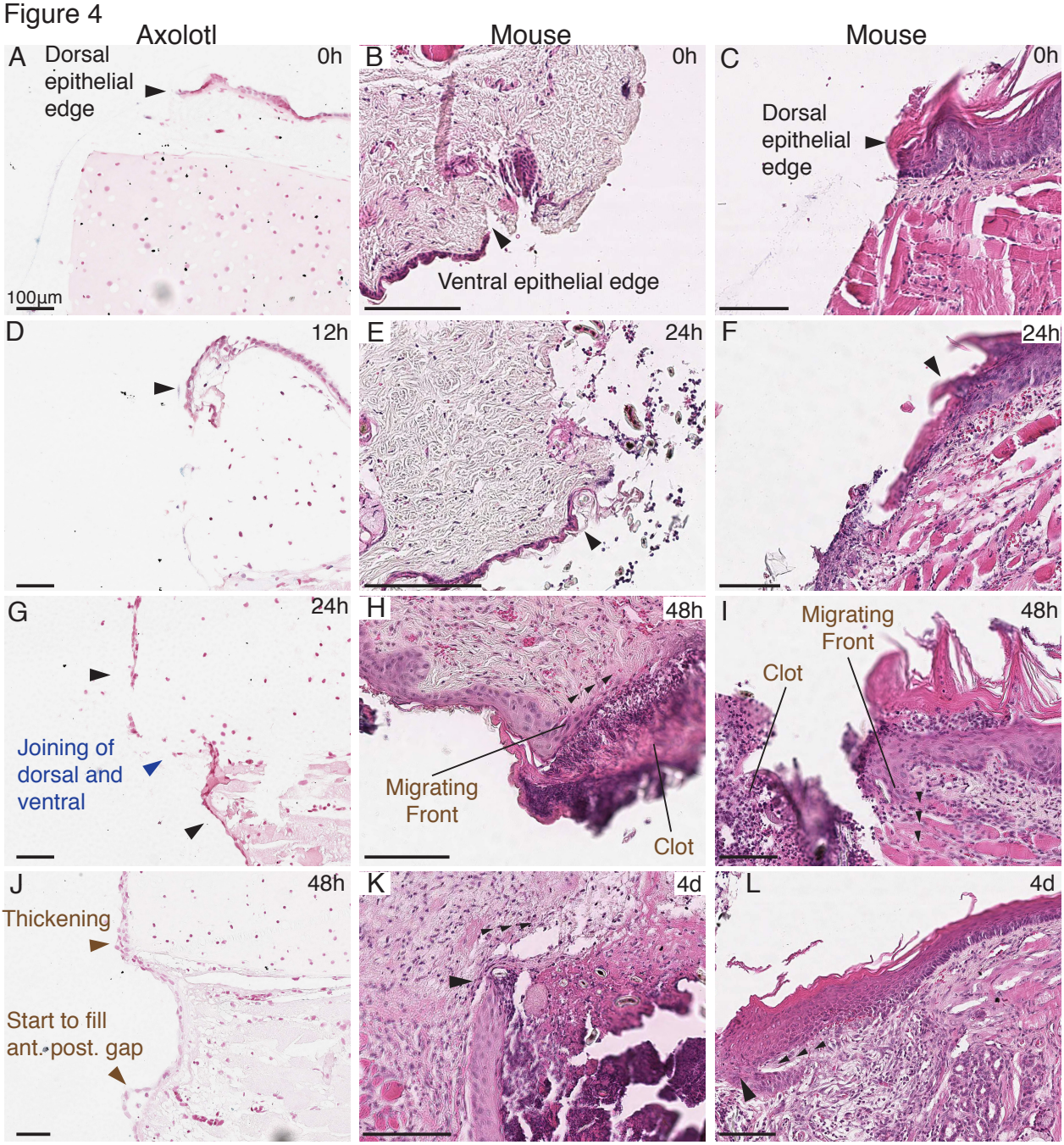
Axolotl
Mouse
Mouse
A
Dorsal epithelial edge
0h
100μm
B
0h
Ventral epithelial edge
C
0h
Dorsal epithelial edge
D
12h
E
24h
F
24h
G
24h
Joining of dorsal and ventral
H
48h
Migrating Front
Clot
I
48h
Migrating Front
Clot
J
48h
Thickening
Start to fill ant.-post. gap
K
4d
L
4d

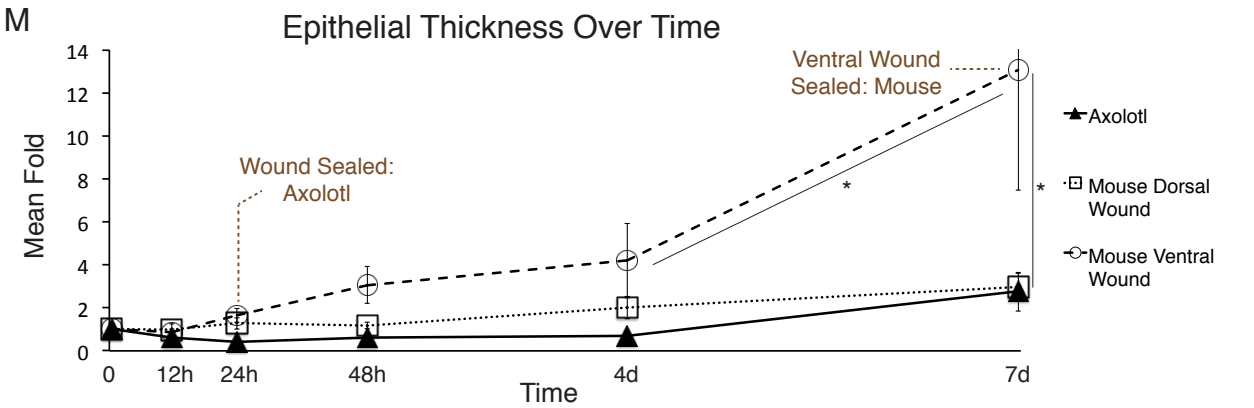
M
Epithelial Thickness Over Time
Mean Fold
14
12
10
8
6
4
2
0
Wound Sealed: Axolotl
Ventral Wound Sealed: Mouse
*
*
0
12h
24h
48h
4d
7d
Time
Axolotl
Mouse Dorsal Wound
Mouse Ventral Wound

Figure 5

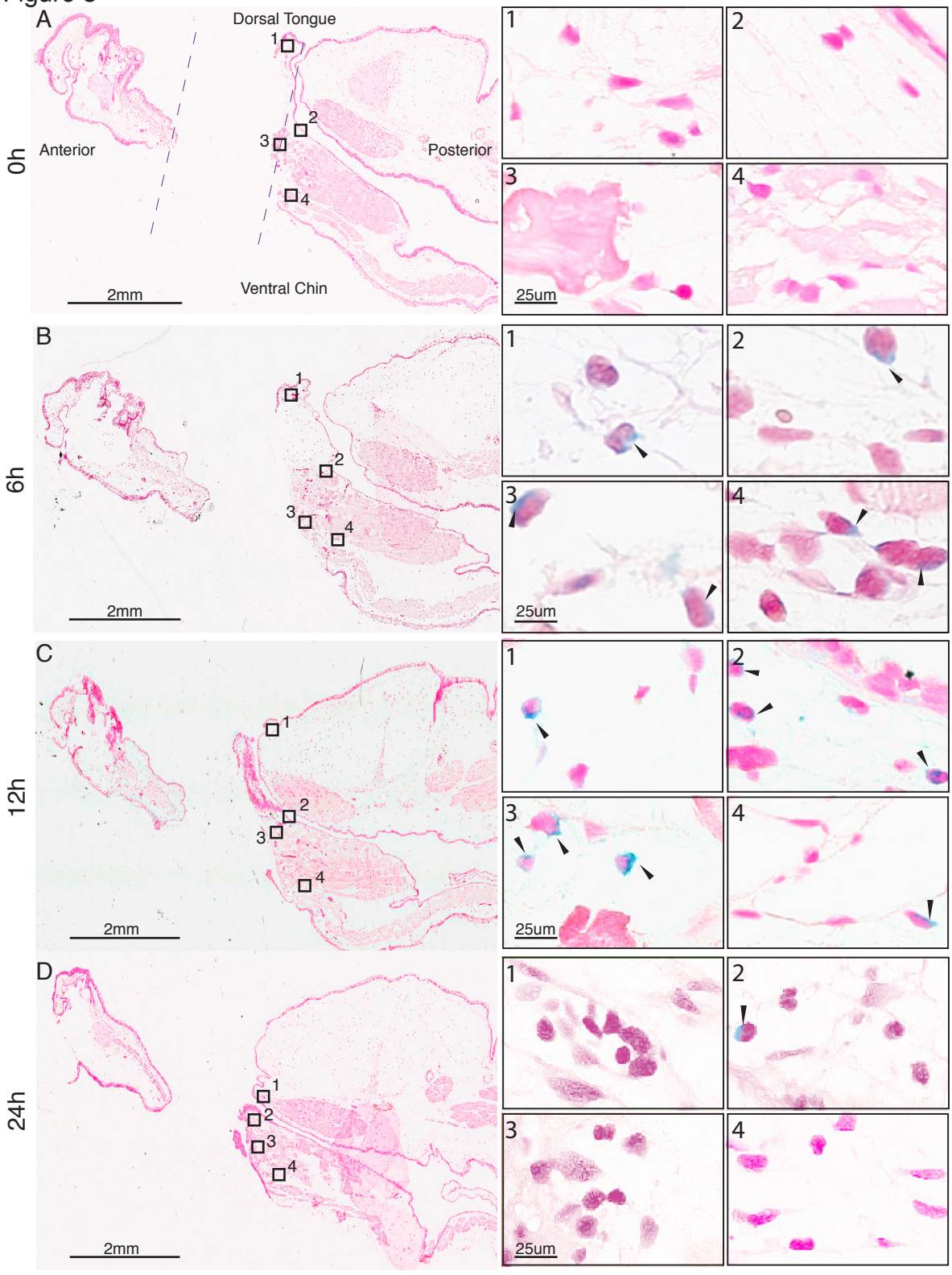
A
Dorsal Tongue
1
2
3
4
Anterior
Posterior
2mm
Ventral Chin
0h
1
2
3
4
25um
B
1
2
3
4
2mm
6h
1
2
3
4
25um
C
1
2
3
4
2mm
12h
1
2
3
4
25um
D
1
2
3
4
2mm
24h
1
2
3
4
25um

Figure 6

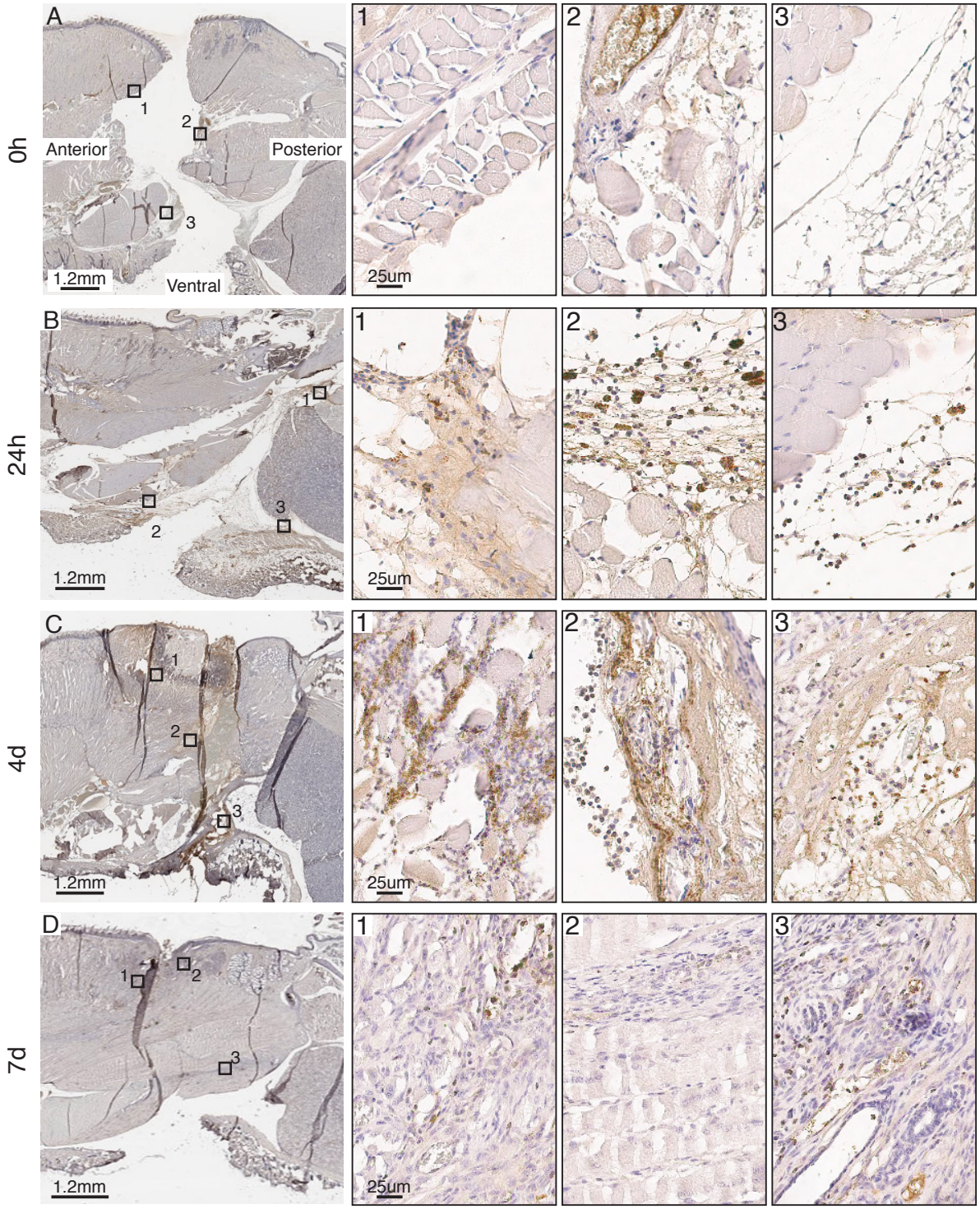

Figure 7

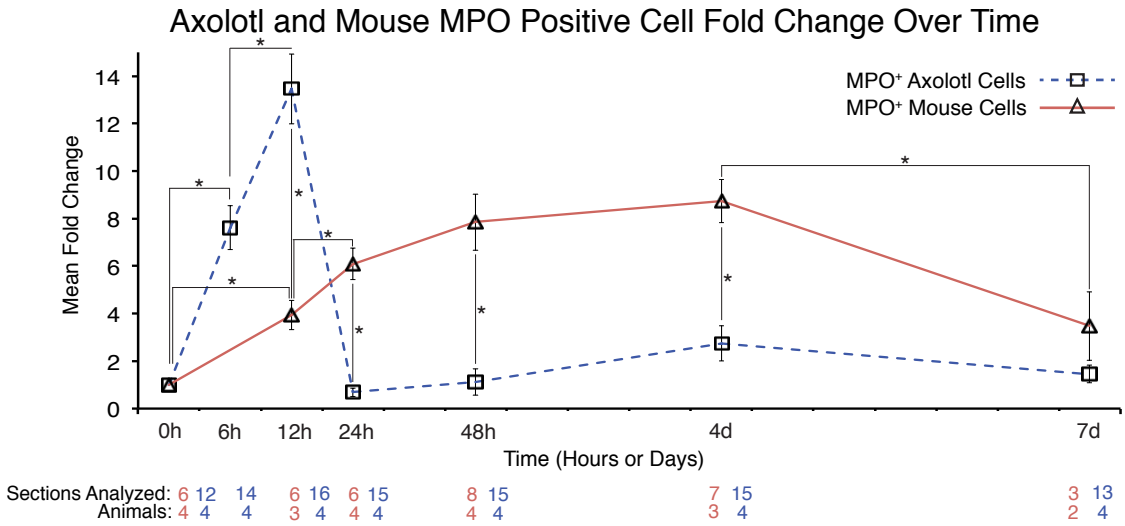
Axolotl and Mouse MPO Positive Cell Fold Change Over Time
MPO+ Axolotl Cells
MPO+ Mouse Cells
Mean Fold Change
0
2
4
6
8
10
12
14
0h
6h
12h
24h
48h
4d
7d
Time (Hours or Days)
Sections Analyzed: 6 12 14 6 16 6 15 8 15 7 15 3 13
Animals: 4 4 4 3 4 4 4 4 4 3 4 2 4

Supplementary Figure 1

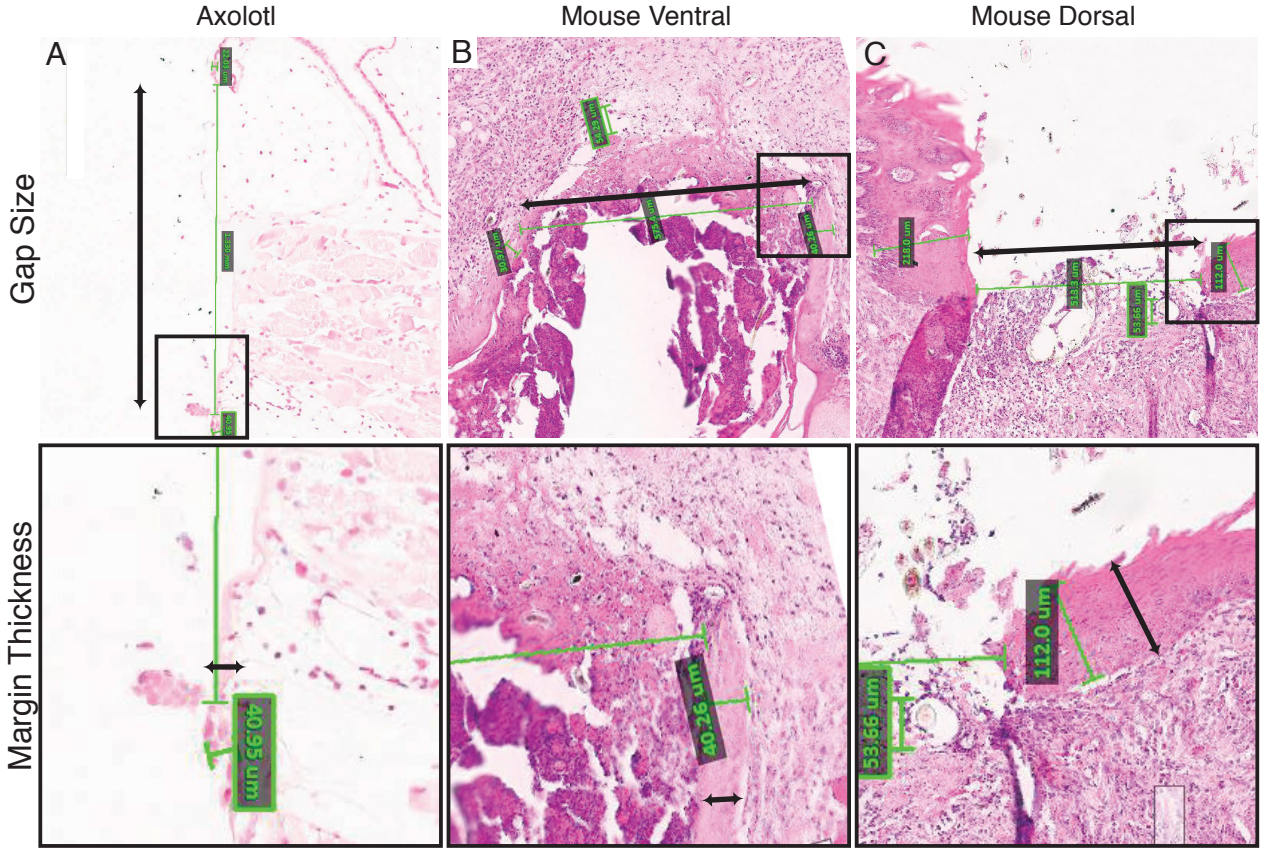

Supplementary Figure 1: Analysis of gap size and epithelial margin thickness. Images are pictures from histologic sagittal sections of the wound. The black boxes are magnifications. Measured distances are parallel to the black line with double arrows. Green lines are also measurement lines while green boxes (or text) show the length of the green line.

Supplementary Figure 2

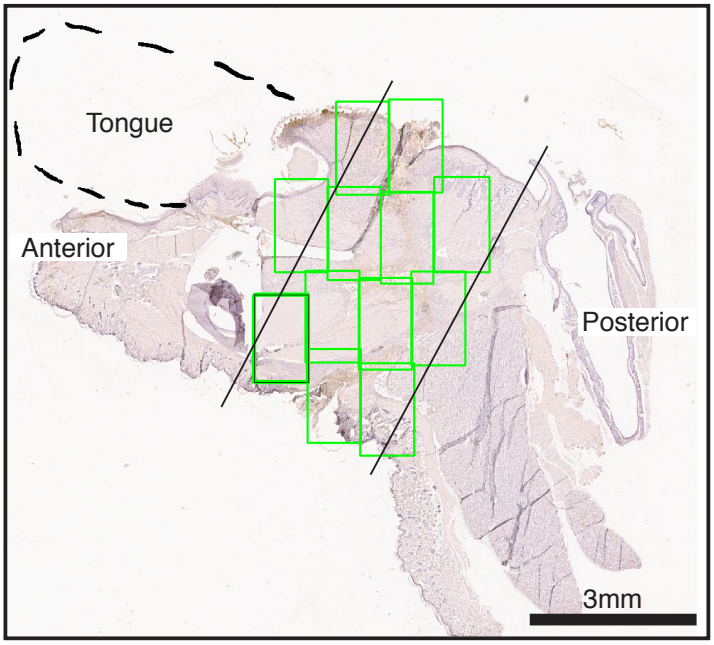

1. Parallel full black lines identify punch biopsy trajectory.

2. Select 12 evenly sized squares (green) around the wound.

3. Take snapshots of the 12 squares.

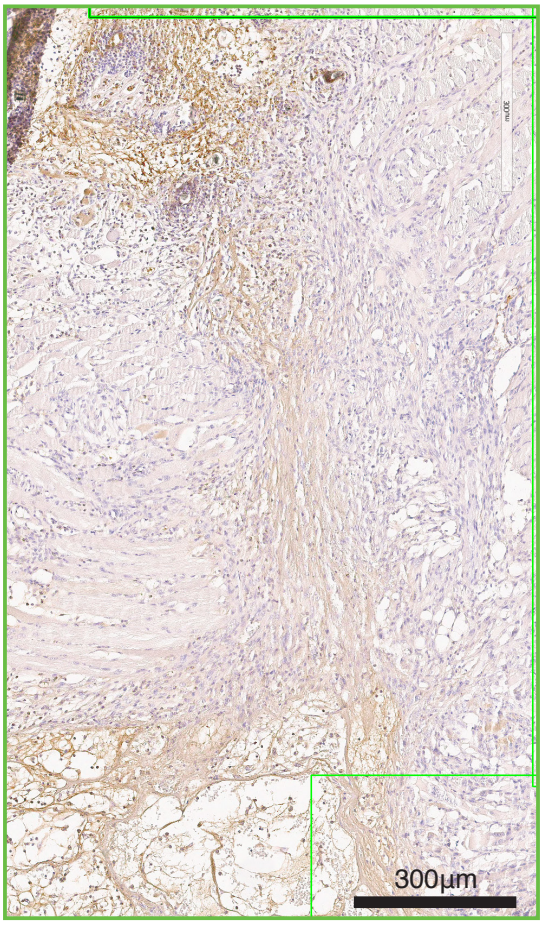

4. Process each snapshot using the detection algorithm.

5. Add up “cell counts” for all 12 images.

6. Totals give brown cell count around wound/section.

Supplementary Figure 2: The image analysis of mouse tissues.

Supplementary Figure 3

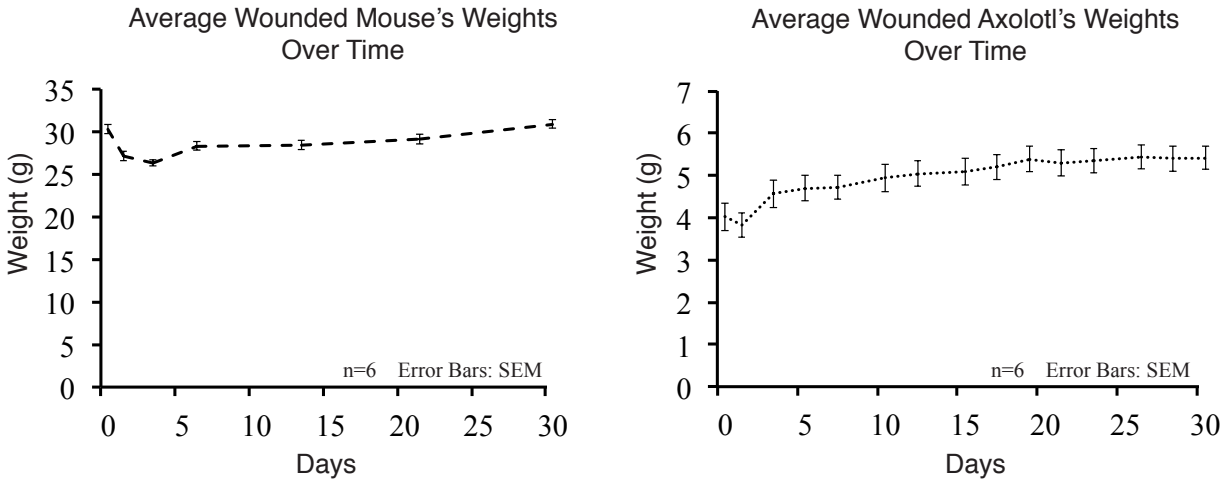

Supplementary Figure 3: Wounded animal's weight over time.

Supplementary Figure 4

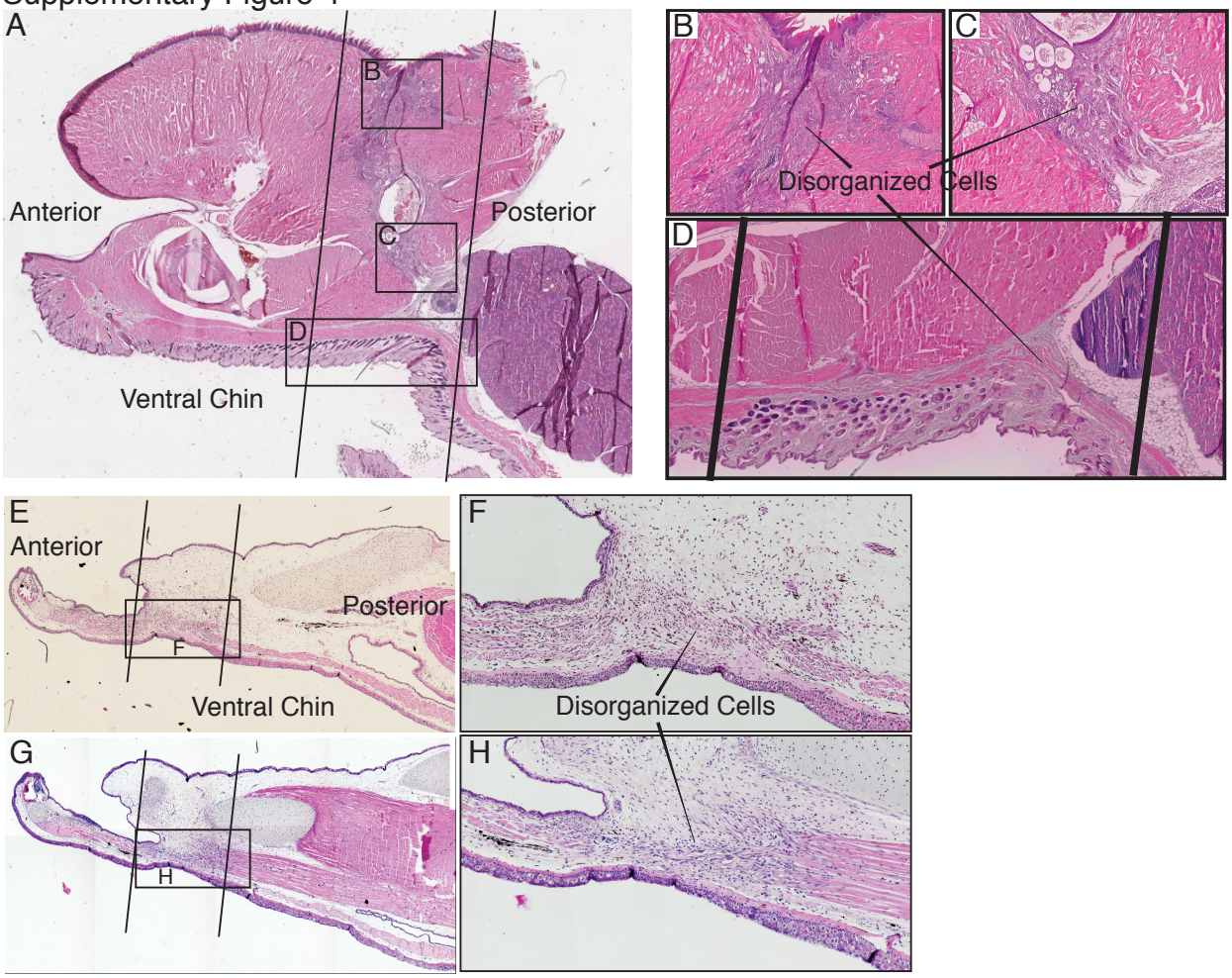

Supplementary Figure 4: Axolotl and mouse have relatively similar healing 30 days after their wound. Images of H&E stained sagittal stained sections from the Mouse and Axolotl 30 days after their wound. Approximate wound punch trajectory in black vertical parallel lines A) Mouse wound at low magnification. B,C,D higher magnification of disorganized cells in mouse tissue. D is from a different animal but same identified location. E,G) Axolot wounds and higher magnification of disorganized cells (F, H).

Supplementary Figure 5

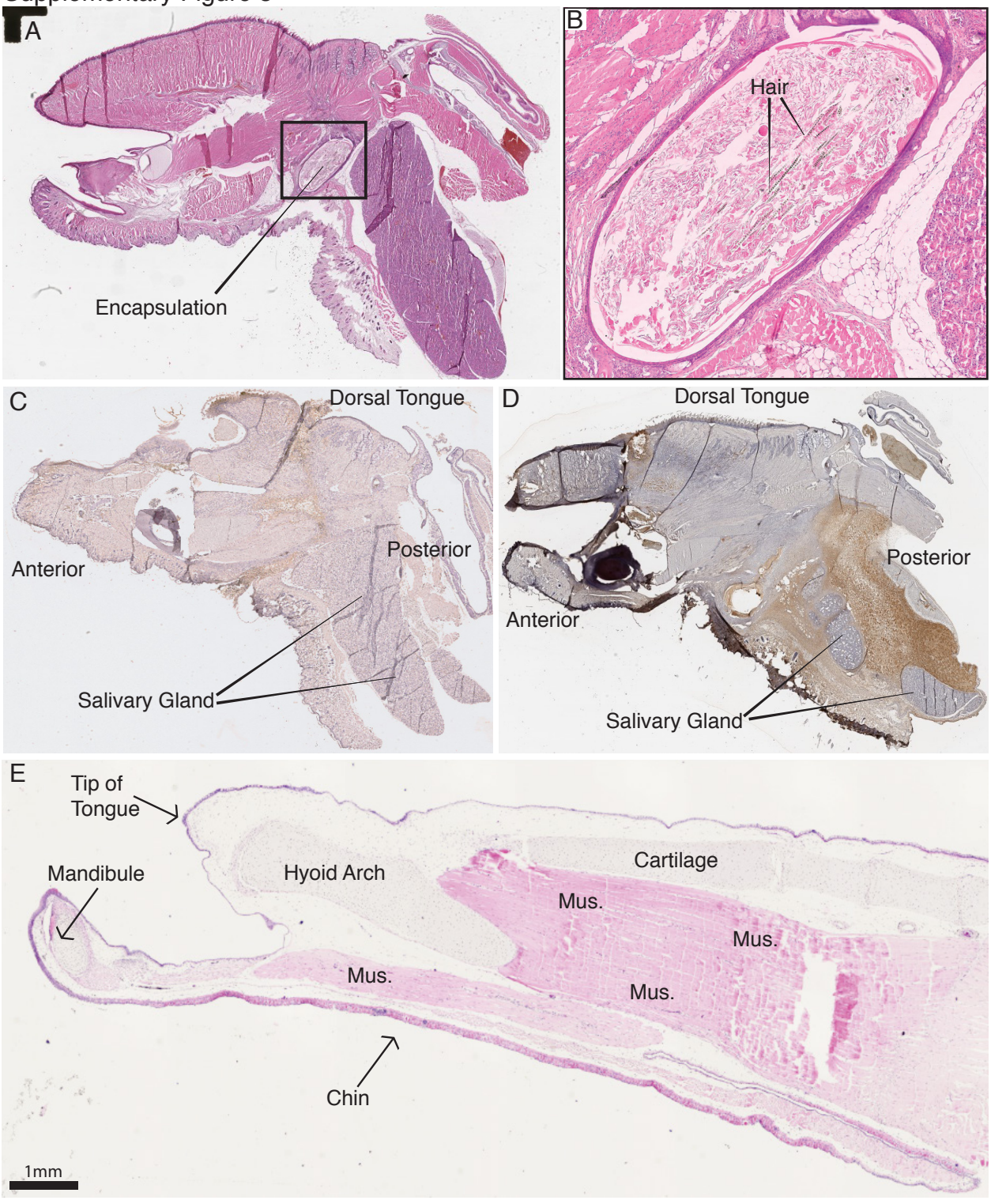

Supplementary Figure 5: Additional histologic observations.A) Wounded mouse lower jaw stained with H&E after 30 days with an encapsulation. B) A higher magnification of the encapsulation showing some animal hair follicles isolated within. C) Mouse lower jaw stained with MPO antibody at 96h. D) This specific animal also stained at 96h had large amounts of MPO positive cells infiltrating the salivary gland. E) H&E sagittal section of unwounded axolotl sagittal section. The section is taken from the middle of the animal's jaw. It is in contrast to the more lateral section shown in Figure 1. In comparison, in these images, the middle of the jaw contains more muscle (Mus.).

Supplementary Information

1. Construction of In-House Mouse Holding Surgical Device

This was made to assist in holding the animal's neck near 90° during the surgery. Two 50 mL conical plastic tubes were thermally cut and fused to create the device. Each tube created a component of the animal's holding device: Tube 1: The lid was removed on one side and the cone on the other side was cut off to create a hollow cylinder; this is where the animal's body rests. Tube 2: Cut to create two open-faced half-pipes. The half-pipe lengths were adjusted and thermally fused at 90°; this is where the animal's neck would bend. Component 2 could be glided onto the hollow cylinder and both could be held together with an elastic. In addition, to prevent the tube from rolling, a well plate lid was also attached to the cylinder with an elastic.

2. Consideration in the Manual and Imaged Based Detection of MPO positive-cell counts.

In the axolotl manual counting, no distance exclusion criteria were used since all MPO positive cells were always found near the wound.

All images representing one animal were subjected to an image analysis algorithm that detected brown nuclei based on the following criteria: 1) Finding brown nuclei with hue, saturation, and intensity, 2) Dilating the pixels that were identified, 3) Indicating average nuclei size for separating clusters, 4) Exclusion based on objects' size.